

# Writhe induced phase transition in unknotted self-avoiding polygons.

E Dagrosa<sup>1</sup>, A L Owczarek<sup>1</sup> and T Prellberg<sup>2</sup>

<sup>1</sup> School of Mathematics and Statistics, The University of Melbourne, Parkville, Vic 3010, Australia.

<sup>2</sup> School of Mathematical Sciences, Queen Mary University of London, Mile End Road, London E1 4NS, UK.

E-mail: e.dagrosa@student.unimelb.edu.au, owczarek@unimelb.edu.au, t.prellberg@qmul.ac.uk

**Abstract.** Recently it has been argued that weighting the writhe of unknotted self-avoiding polygons can be related to possible experiments that turn double stranded DNA. We first solve exactly a directed model and demonstrate that in such a subset of polygons the problem of weighting their writhe is associated with a phase transition. We then analyse simulations using the Wang-Landau algorithm to observe scaling in the fluctuations of the writhe that is compatible with a second-order phase transition in a undirected self-avoiding polygon model. Crucially, we conclude that the transition becomes apparent when the polygon is stretched sufficiently with a pulling force.

## 1. Introduction and Model

Over the past two decades, experiments [1, 2, 3, 4, 5, 6, 7] that turn single molecules of twist-storing polymers like DNA have been performed. The conformational transition that is associated with these experiments attracts continuing interest. In this paper, we propose a related thought experiment and model it by weighting the writhe of self-avoiding polygons (SAP) on the simple cubic (sc) lattice. We are interested in observing the typical signs that are associated with real phase transitions.

### 1.1. The SAW as model of phase transitions

The self-avoiding walk (SAW) in three dimensions is one of the simplest models of polymers. It reduces polymers down to two features. First, it represents the fact that a polymer is composed from a large number of repeating subunits. Second, the self-avoidance reflects the fact that polymers cannot be compressed arbitrarily. As a model of long polymers in statistical mechanics, the SAW is known to make correct predictions about the scaling of the end-to-end distance or equivalently the radius of gyration of a polymer in a good solvent at thermal equilibrium. When we denote the length of the

SAW by  $n$ , the expectation value of the squared radius of gyration is predicted to obey the scaling form

$$\langle R_g^2 \rangle_n = A_g n^{2\nu} (1 + b_g n^{-\Delta} + \dots) \quad (1.1)$$

where  $A_g$  and  $b_g$  are constants specific to the lattice on which the SAW lives. In contrast, the exponents  $\nu$  and  $\Delta$  are considered to be universal. They have been determined from simulations [8] as well as from calculations in the context of the renormalization group idea. This is due to a mapping of the SAW onto the magnetic  $N$ -vector model in the formal limit  $N \rightarrow 0$ . Recent predictions [9] are  $\nu = 0.587597 \pm 0.000007$  and  $\Delta = 0.528 \pm 0.012$ . The predictions for the leading scaling exponent  $\nu$  agree with experiments on DNA [10] that for long molecules of DNA fit their results to  $\langle R_g \rangle \sim L^\nu$ , where  $L$  is the length of the DNA.

In addition SAWs are used as configurations of various standard models of single polymer phase transitions. Most notable are the collapse and adsorption transitions. In the latter case, one considers all SAWs above a plane in three dimensions or above a line in two dimensions and weights the SAWs by the number of contacts made with the wall (surface or line, respectively). Denote a SAW by  $\varphi = \{\varphi_i\}_{i=1,\dots,n+1}$ , where  $\varphi_i$  are the vertices. Denote by  $a$  the number of visits to the wall, then the SAWs of length  $n$  are distributed according the Boltzmann distribution

$$p(\varphi) = Z_n^{-1} e^{\beta_a a(\varphi)}, \quad (1.2)$$

where  $a(\varphi)$  measures the number of visits in  $\varphi$ ,  $Z_n = \sum_{\varphi \in \Omega_n} e^{\beta_a a(\varphi)}$  is the partition function and  $\beta_a$  is related to the interaction strength between the polymer and the wall. We remark that we use the subscript in the coupling  $\beta_a$  only as a label, not an index so that when we denote by  $C_{na}$  the number of SAWs of length  $n$  with  $a$  visits, we may write the partition function as

$$Z_n(\beta_a) = \sum_a C_{na} e^{\beta_a a}. \quad (1.3)$$

The finite size free energy is defined as  $f_n(\beta_a) = n^{-1} \log Z_n(\beta_a)$  so that in the thermodynamic limit  $n \rightarrow \infty$ , it is known that there is a critical value  $\beta_a^{(\infty)}$  at which the free energy  $f = \lim_{n \rightarrow \infty} f_n$  becomes non-analytic. When the critical value is crossed from below the system undergoes a continuous phase transition from a desorbed phase into the adsorbed phase. In the desorbed phase the first derivative of the free energy with respect to  $\beta_a$  vanishes, while in the adsorbed phase a certain fraction of the vertices is expected to be in contact with the wall. Correspondingly, the transition is associated with a discontinuity in the second derivative  $\partial^2 f(\beta_a) / \partial \beta_a^2$ , which jumps from zero to some finite value at  $\beta_a^{(\infty)}$ . At finite size, the singular part of the free energy near  $\beta_a^{(\infty)}$  obeys a standard scaling Ansatz

$$f_n^{(sing)}(\tau) = n^{-1} h(n^\phi \tau). \quad (1.4)$$

where  $\tau = \beta_a - \beta_a^{(\infty)}$ ,  $h(x)$  is a scaling function and  $\phi$  is called the crossover exponent. In the case of the adsorbed walk, the crossover exponent takes a mean field value of  $1/2$  at the transition. An exact solution for certain directed SAWs in two dimensions is given in [11], which also includes an expression for the scaling function. In the following, we will consider SAP which are SAWs, the first and last vertex of which are adjacent.

### 1.2. The Writhe of SAPs on the sc lattice

The writhe is a quantity associated with the topology and geometry of a space curve. In the lattice polymer literature [12, 13, 14, 15, 16], the writhe of a SAP is usually computed based on a theorem by Lacher and Sumners [17, 18], who realized that the expression for the writhe of a  $C^1$  curve  $R$

$$Wr(R) = \frac{1}{4\pi} \int_{S^2} d\mathbf{d} Lk(R, R + \epsilon \mathbf{d}) \quad (1.5)$$

simplifies for a SAP  $\varphi$  on the sc lattice to considering the linking number between  $\varphi$  and four copies of  $\varphi$  that are translated by eg.  $\mathbf{d} = (\pm 1/2, \pm 1/2, 1/2)^T$ . Therefore,

$$Wr(\varphi) = \frac{1}{4} \left\{ Lk\left(\varphi, \varphi + \frac{1}{2}(1, 1, 1)^T\right) + Lk\left(\varphi, \varphi + \frac{1}{2}(1, -1, 1)^T\right) + \dots \right\}. \quad (1.6)$$

On the other hand, there exist several [19, 20] expressions for the writhe of polygonal curves. In [21] we derived one of these ourselves. When the  $N$  segments of a polygonal knot  $R$  are aligned in directions  $\hat{\mathbf{a}}_i$   $i = 1, \dots, N$ , the writhe is given by

$$Wr(R) = Lk(R, R + \epsilon \mathbf{d}) - \sum_{i=1}^N Tw_i(\mathbf{d}), \quad (1.7)$$

with

$$Tw_i(\mathbf{d}) = \frac{\text{sgn}([\hat{\mathbf{a}}_{i-1}, \hat{\mathbf{a}}_i, \mathbf{d}])}{2\pi} \left\{ \arctan\left(\frac{\langle \mathbf{d}, \hat{\mathbf{a}}_{i-1} \rangle - \langle \mathbf{d}, \hat{\mathbf{a}}_i \rangle \langle \hat{\mathbf{a}}_{i-1}, \hat{\mathbf{a}}_i \rangle}{|[\hat{\mathbf{a}}_{i-1}, \hat{\mathbf{a}}_i, \mathbf{d}]|}\right) + \arctan\left(\frac{\langle \mathbf{d}, \hat{\mathbf{a}}_i \rangle - \langle \mathbf{d}, \hat{\mathbf{a}}_{i-1} \rangle \langle \hat{\mathbf{a}}_{i-1}, \hat{\mathbf{a}}_i \rangle}{|[\hat{\mathbf{a}}_{i-1}, \hat{\mathbf{a}}_i, \mathbf{d}]|}\right) \right\}, \quad (1.8)$$

where  $\hat{\mathbf{d}}$  must be chosen so that it does not lie on the tantrix of  $R$ . (The tantrix, or tangent indicatrix, is the set of all unit tangents to the curve.) We can then apply (1.7) to a general SAP on the sc lattice to obtain

**Lemma 1.** *Let  $\mathbf{d} = (1, 1, 1)$ , then the writhe of a SAP  $\varphi$  on the sc lattice is given by*

$$Wr(\varphi) = Lk(\varphi, \varphi + \epsilon \mathbf{d}) - \frac{1}{8} \sum_{i=1}^n [\hat{\varphi}_{i-1}, \hat{\varphi}_i, \mathbf{d}] \langle \mathbf{d}, \hat{\varphi}_{i-1} + \hat{\varphi}_i \rangle. \quad (1.9)$$

*Proof.* In (1.7), the segment directions  $\hat{\mathbf{a}}_i$  take the values of one of the lattice vectors  $\hat{\mathbf{a}}_i = s_i \hat{\mathbf{k}}_i$  of the sc lattice ( $\hat{\mathbf{k}}_i \in \{(1, 0, 0)^T, (0, 1, 0)^T, (0, 0, 1)^T\}$ ). Here  $s = \pm 1$  stands for sign. When we use the bond directions  $\hat{\varphi}_i = \varphi_{i+1} - \varphi_i$  rather than the segment directions  $\hat{\mathbf{a}}_i$ , we have to distinguish two cases. In the first case the incoming and outgoing step of vertex  $\varphi_i$  are in the same direction, so that the vertex is part of a longer segment and we have  $Tw_i = 0$ . The other case is,  $\langle \hat{\varphi}_{i-1}, \hat{\varphi}_i \rangle = 0$ , so that

$$\begin{aligned} [\hat{\varphi}_{i-1}, \hat{\varphi}_i, \mathbf{d}] &= \pm 1, \\ \langle \mathbf{d}, \hat{\varphi}_i \rangle &= s_i, \end{aligned} \tag{1.10}$$

therefore

$$\begin{aligned} Tw_i &= \frac{\text{sgn}([\hat{\varphi}_{i-1}, \hat{\varphi}_i, \mathbf{d}])}{2\pi} (\arctan(s_{i-1}) + \arctan(s_i)) \\ &= \frac{[\hat{\varphi}_{i-1}, \hat{\varphi}_i, \mathbf{d}]}{8} (s_{i-1} + s_i). \end{aligned} \tag{1.11}$$

Therefore, when  $s_i$  and  $s_{i-1}$  have different signs,  $Tw_i = 0$ , otherwise  $Tw_i = \pm 1/4$  (used  $\arctan(\pm 1) = \pm \pi/4$ ). Then, the lemma follows from (1.7).  $\square$

The ensemble of SAPs on the sc lattice has been considered in [12], where the authors introduced a scaling exponent  $\zeta_w$  associated with the absolute writhe. Here, we will define this exponent via the relation

$$\langle w^2 \rangle_n = A_w n^{2\zeta_w} + o(n^{2\zeta_w}). \tag{1.12}$$

The results obtained in [12, 13] via simulations are compatible with  $2\zeta_w = 1$ , which in [12] was suspected to be the lower boundary for  $2\zeta_w$ . In [13], it was shown via simulations that the value  $2\zeta_w = 1$  appears to hold even when the ensemble is restricted to SAPs of given knot types (Figure 1.1). We point out that the fits used to estimate the scaling exponent from simulation results did not take into account any corrections to the leading scaling in (1.12) and all fits that have been performed consistently estimated  $2\zeta_w$  slightly larger than one. For SAWs (not SAPs), it was shown in [22] via the renormalization group method that  $2\zeta_w = 1$ . It was also determined that the corrections  $o(n^{2\zeta_w})$  take the form  $-B_w \log n$  at the collapse transition.

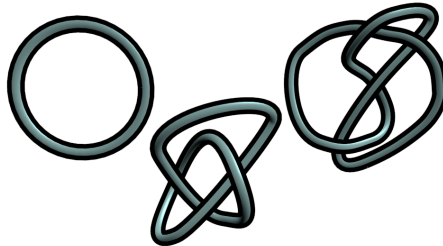


**Figure 1.1.** Diagrams of prime knots. The knot types are: the unknot, the trefoil knot and the  $4_1$  knot.

In a previous paper [23] we have considered the partition function  $Z(\beta_l) = \sum C_{nw} e^{\beta_l w}$ , where we weight the writhe of SAWs using simulations, but without restricting the knot type. We found a strong first-order transition, which had been suspected by [24, 22] using renormalization group arguments. We showed that this first-order transition is between different knot types, so that at high  $\beta_l$  the ensemble is dominated by complicated chiral knots near maximum writhe. We remark that the results provided in [25] should imply that for a general SAW on any lattice the maximum writhe scales as  $Wr_n^{(max)} = \text{const } n^{4/3}$ , so that we would expect  $2\zeta_w = 8/3$  at high  $\beta_l$ .

However, when the knot type is restricted, the maximum writhe will be bounded as  $Wr_n^{(max)} \sim n$ . Therefore, at high  $\beta_l$  one expects  $2\zeta_w = 2$ . The formula (1.7) suggests that the writhe can be decomposed into a global and local contribution. However, this decomposition is not unique as it depends on the choice of  $\mathbf{d}$ . Nevertheless, it is possible to consider an ensemble of SAWs (SAPs), such that for every state of the ensemble all writhe can be computed along the SAW. For example, one can weight the writhe of directed SAWs that form the center line of a directed lattice ribbon [26]. Due to its local nature, this model is not associated with a phase transition as the free energy for large  $n$  will take the form  $f_n(\beta_l) = f_0(\beta_l) + g_n(\beta_l)$  with  $\lim_{n \rightarrow \infty} g_n = 0$ . Due to symmetry of the writhe, that is  $C_{nw} = C_{n-w}$ , the writhe expectation value ( $n \frac{\partial f_n(\beta_l)}{\partial \beta_l}$ ) vanishes at  $\beta_l = 0$ . Then with

$$\langle w^2 \rangle_n = n \frac{\partial^2 f_n(\beta_l)}{\partial \beta_l^2} + n^2 \left( \frac{\partial f_n(\beta_l)}{\partial \beta_l} \right)^2, \quad (1.13)$$

the scaling exponent must take the form

$$2\zeta_w(\beta_l) = \begin{cases} 1 & \beta_l = 0, \\ 2 & \beta_l \neq 0. \end{cases} \quad (1.14)$$

We can consider the values of  $\zeta_w$  in (1.14) to be trivial as they can be understood by writhe forming along the SAW/SAP.

### 1.3. Twist Storing Polymers

Polymers that can absorb energy in the form of twist have been called [27] twist-storing polymers. Most prominently, this includes double stranded DNA. Experiments [1, 2, 3, 4, 5, 6, 7] performed on dsDNA in thermal equilibrium resemble turning a piece of rubber coated cable. After adding sufficient turns to the molecule, the polymer is believed to undergo a transition into states in which it wraps around itself to form plectonemes. In the literature [27, 28, 29, 30, 31, 32, 33] the mechanics of this have been modeled as ribbons [28, 34, 35, 36]. The boundary curves of the ribbon can (for example) be thought to represent the strands of a DNA molecule. Only if the knot type (Figure 1.1) of the polymer is conserved, the linking number between these curves is controlled by the number of turns and according to the CFW theorem [28, 34, 35, 36], the linking number can be absorbed either in the form of twist or in the form of writhe:

$$Lk = Wr + Tw. \quad (1.15)$$

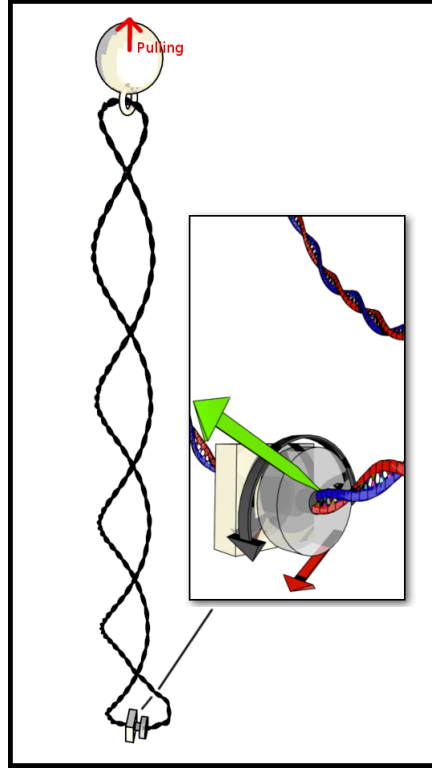


**Figure 1.2.** Sketch of the thought experiment. Both sides of a DNA like polymer are attached to the apparatus. The depicted cylinder can be rotated (black arrows). The TSP exerts a force  $f$  on the cylinder which attacks at a distance  $r$  from the centre (green arrow). On the other hand, a force  $F$  (red arrow) can be applied at a distance  $R$  from the centre. Then, the net torque exerted on the cylinder reads  $FR - fr$ .

In this paper we devise a thought experiment that is slightly different from the ones currently performed on DNA. We consider a two sided apparatus as shown in Figure 1.2. On one side the twist storing polymer (TSP) is attached to an immobile part of the apparatus, on the other side, the TSP is connected to a turn-able cylindrical structure, which is used to control the linking number between the two strands of the double stranded molecule. In order to apply a pulling force, we take a magnetic bead, attach a loop to it and pass one end of the TSP through the loop before it is attached to the apparatus. Via a magnetic field, a constant pulling force can be applied to the polymer. Note that the force does not attack at a specific point of the TSP. In fact, it is important that there is as little as possible interaction between the loop material and the TSP. Instead of controlling the number of turns, we can imagine to keep the polymer at a constant torque  $\beta_l$ . This is called the constant torque ensemble.

#### 1.4. Model: Self-Avoiding Unknot on the sc lattice

We conjecture that the critical structure related to the above thought experiment can be obtained by weighting the writhe of self-avoiding polygons on the sc lattice. This is supported by the observation that the linking number of a lattice ribbon was recently

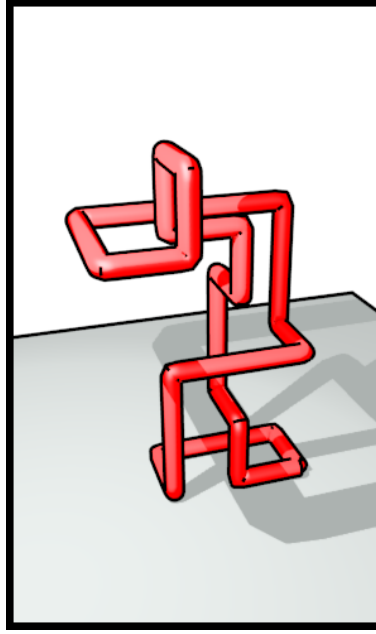


**Figure 1.3.** A self-avoiding unknot (SAUK) above a surface of length  $n = 28$ . The step furthest away from the surface defines the extension  $h$ .

proved to be equal to the writhe of the centre line of the lattice ribbon in [21], itself a self-avoiding polygon on the sc lattice. While not every self-avoiding polygon on the simple cubic lattice can be the center line of the lattice ribbon, the condition for polygons that can is merely local, so that we conjecture that the critical structure remains unaffected by extending the ensemble to all SAPs. The knot type of these polymers is restricted to be the unknot. Thus, we refer to these as self-avoiding unknots (SAUK). Imagine a surface at  $x_3 = 0$ , so that the SAUK is restricted to the positive half space  $(\varphi_i)_3 \geq 0$ . In the thought experiment, the energy associated with pulling is proportional to the distance  $h$  of the bead from the plane  $x_3 = 0$ . At least for strong pulling forces this should typically be identical to the  $x_3$ -component of the vertex furthest away from the surface. We define

$$h = \max_{i=1,\dots,n} (\varphi_i)_3. \quad (1.16)$$

The second parameter  $w$  is an appropriate multiple of the writhe. Then, the partition function reads

$$Z_n(\beta_l, \beta_h) = \sum_{w,h} C_{nwh} e^{\beta_l w + \beta_h h}, \quad (1.17)$$

where  $C_{nwh}$  is the number of SAUKs of length  $n$ , writhe  $w$  and extension  $h$ . The finite size free energy is given by  $f_n(\beta_l, \beta_h) = n^{-1} \log Z_n(\beta_l, \beta_h)$ .

### 1.5. Overview

The remainder of this paper is structured as follows. In Section 2 we will define a directed version of a SAUK. We use it to show via an exact solution that weighting

the writhe of certain unknotted induces a real phase transition. By construction, this transition must be associated with the SAUK wrapping around itself. In Section 3 we use simulations to weight the writhe of pulled SAUK on the sc lattice. We summarize and discuss the results in Section 4.

## 2. Directed unknotted SAP with Axis

In this section, we define a directed version of a SAP on the sc lattice, the knot type of which is the unknot. When a general unknotted SAP is under strong stretching force and not too much torque, we might expect that a typical conformation may be approximated by two SAWs, directed in pulling direction, that begin at the origin and join on some plane  $x_3 = h$ . The directedness of the SAWs guarantees that the joined object is indeed an unknot. Unfortunately, this model is still too hard to solve so that we will have to simplify it considerably. Therefore, consider that one of the two SAWs steps only along a given axis. The resulting object shall be called a self-avoiding unknot (SAUK) with axis.

**Definition 1.** Given a lattice base vector  $\hat{\mathbf{k}}$  on the sc lattice and a root vertex  $\varphi_1$ , we define an SAUK with axis  $\varphi$  of length  $n$  as a two component lattice object. The first component is a directed self-avoiding walk comprising of vertices  $\varphi_1, \varphi_2, \dots, \varphi_m$  such that

- (i) The walk ends on the axis defined by  $\hat{\mathbf{k}}$  and the root, i.e.  $\varphi_m = \varphi_1 + (n - m + 1) \hat{\mathbf{k}}$
- (ii) No vertex of the walk except  $\varphi_1$  and  $\varphi_m$  lie on the axis, i.e.  $\varphi_i \neq \left( \varphi_1 + j \hat{\mathbf{k}} \right)$  for all  $j \in \mathbb{N}$  and all  $i = 2, \dots, m - 1$ .
- (iii) The walk is directed and makes no steps against the  $\hat{\mathbf{k}}$  direction, i.e.  $(\varphi_{i+1} - \varphi_i) \cdot \hat{\mathbf{k}} \geq 0$  for all  $i = 2, \dots, m - 1$

The second component is a walk of length  $n - m$  that connects the vertices  $\varphi_m$  and  $\varphi_1$ . The vertex positions are given as  $\varphi_i = \varphi_1 + (n - i + 1) \hat{\mathbf{k}}$   $i = m + 1, \dots, n - 1$ .

The general case of SAUKs with axis is still too hard to solve, so that only a subset of SAUKs with axis on the sc lattice will be considered for the ensemble. Their construction is described in the following. The axis direction will be  $\hat{x}_3$  and the lattice polymer will be confined to the slab  $-1 \leq x_2 \leq 1$ . We set  $\varphi_1 = (0, 0, 0)$ ,  $\varphi_2 = (0, -1, 0)$ ,  $\varphi_3 = (0, -1, 1)$ ,  $\varphi_n = (0, 0, 1)$ . The SAUKs can be constructed by appending double steps in  $(\pm \hat{x}_1) \hat{x}_3$  direction. For example, we can append a double step  $\hat{x}_1 \hat{x}_3$  to  $\varphi_3$  so that  $\varphi_4 = (1, -1, 1)$  and  $\varphi_5 = (1, -1, 2)$ . In addition, whenever the current  $x_1$ -component is not zero, a triple step  $\hat{x}_2 \hat{x}_2 \hat{x}_3$  or  $(-\hat{x}_2)(-\hat{x}_2) \hat{x}_3$  can be appended. The applicable step combination depends on whether the current vertex lies on the plane  $x_2 = -1$  or  $x_2 = 1$ . With every appended double or triple step, we also append a step in  $(-\hat{x}_3)$  direction to the axis. Whenever a vertex with components  $(0, -1, n_3 \in \mathbb{Z})$  is reached, the SAUK can be finished by appending a step in  $\hat{x}_2$ -direction. A lattice object constructed according to these rules is shown in Figure 2.1. We can choose the writhe formula (1.9), to find the rule that the double steps in  $\hat{x}_2$  direction contribute 1 to writhe  $w = Wr$  when



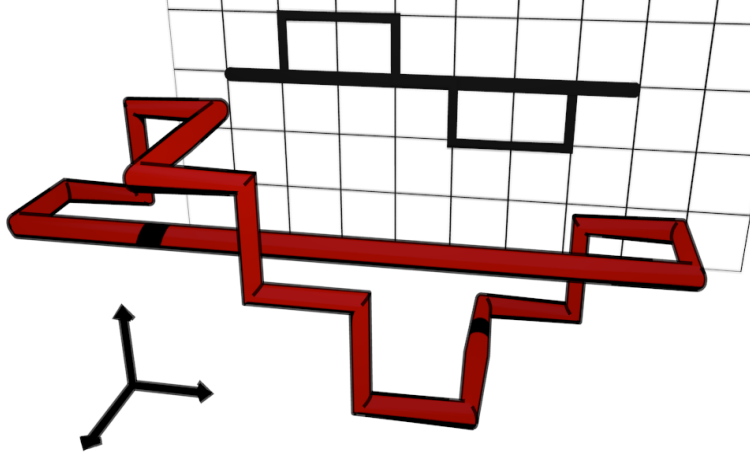


**Figure 2.1.** SAUK with axis of length 24. The depicted case is an additionally directed version, which can be (more or less) solved exactly.

$x_1 > 0$ , and the double steps in  $-\hat{x}_2$  direction decrease the writhe by 1. When  $x_1 < 0$ , the writhe contributions are inverted. From this point of view, there is no other source of writhe. Note that the writhe of this simplified SAUK with axis comes in multiples of two. We do not consider a pulling force, so that when we denote the number of these specified SAUKs with length  $n$  and writhe  $w$  by  $C_{nw}$  the partition function reads

$$Z_n(\beta_l) = \sum_w C_{nw} e^{\beta_l w}. \quad (2.1)$$

To solve the model, we will try to obtain an expression for the generating function of SAUKs with axis

$$\bar{a}(\beta_l, z) := \sum_n Z_n(\beta_l) z^n. \quad (2.2)$$

The strategies for solving similar problems have been used for example in [37, 38]. In addition to the generating function 2.2, one introduces a generating function for unfinished SAUKs of length  $n$ , where  $n$  counts the number of steps in the walk and in the axis. Denote by  $a_h$  the generating function of unfinished SAUKs whose walk ends on the plane  $x_2 = -1$  at  $x_1 = h$ . Correspondingly, when the walk ends on the plane  $x_2 = 1$ , we denote the generating function by  $b_h$ . Therefore,  $\bar{a}(\beta_l, z) = z a_0(\beta_l, z)$ . Define  $y_l = \exp\{\beta_l\}$ , and with

$$\Theta(x) = \begin{cases} 1 & x > 0, \\ 0 & x \leq 0, \end{cases}$$

define

$$H_h(y_l) := \{y_l^{-1} \Theta(h) + y_l \Theta(-h)\}. \quad (2.3)$$

Note that  $H_{-h} = 1/H_h$  (when  $h \neq 0$ ) and  $H_0(y_l) = 0$ . Then, the recursion relations for the generating functions read

$$a_h = z^3 (\delta_{h,0} + a_{h+1} + a_{h-1}) + z^4 H_h b_h, \quad (2.4)$$

and

$$b_h = z^3 (b_{h+1} + b_{h-1}) + z^4 H_{-h} a_h. \quad (2.5)$$

The factors  $z^3$  and  $z^4$  correspond to double and triple steps, respectively. The additional factor of  $z$  is associated with the additional reverse step on the axis. For  $h = 0$ , the generating function  $a_0$  also contains the initial configuration formed by three steps. The goal is to obtain  $a_0$  and to get rid of all the  $b_h$ . Note that for  $h \neq 0$  (2.8) can be inverted to give

$$b_h = z^{-4} H_{-h} \{a_h - z^3 (a_{h+1} + a_{h-1})\}. \quad (2.6)$$

For  $|h| > 1$ , this can be used in (2.5) to obtain the bulk relation for  $a_h$ ,

$$0 = z^6 a_{h-2} - 2z^3 a_{h-1} + (1 + 2z^6 - z^8) a_h - 2z^3 a_{h+1} + z^6 a_{h+2}. \quad (2.7)$$

This is a difference equation of order four for  $a_h$ . The general solution has the form  $a_h = \sum_{i=1}^4 C_i \lambda_i^h$ , where  $\lambda_i$  are the roots of the characteristic equation to (2.7). The series expansion of the solutions yields  $\lambda_1 = 1/\lambda_2 = z^3 + z^7 + z^9 + O(z^{11})$  and  $\lambda_3 = 1/\lambda_4 = z^3 - z^7 + z^9 + O(z^{11})$ . The solutions with the alternating sign in the expansion are incompatible with a generating function (i.e.  $Z_n > 0$ ) so that the solution must take the form

$$a_h = C^+ \lambda_+^h \Theta(h) + C^- \lambda_-^h \Theta(-h) \quad (2.8)$$

with

$$\lambda_{\pm}(z) = \frac{1}{2z^3} (1 - z^4 \mp R(z)), \quad (2.9)$$

where  $R(z) = \sqrt{1 - 2z^4 - 4z^6 + z^8}$  and  $\lambda_+ \lambda_- = 1$ . It follows from the series expansions that  $\lambda_+$  applies for  $h > 0$  and  $\lambda_-$  for  $h < 0$ .

With  $r = \sqrt{\frac{1}{3} \left\{ 3 - \frac{2 \cdot 6^{2/3}}{(-9 + \sqrt{129})^{1/3}} + (6(-9 + \sqrt{129}))^{1/3} \right\}}$ , the solution (2.8) has a square root singularity at

$$z_b = \frac{1}{2} \left( \sqrt{3 + \frac{2}{r} - r^2} - 1 - r \right) \approx 0.717. \quad (2.10)$$

Therefore  $R(z_b) = 0$  and  $z_b$  can be associated with the bulk phase. For  $|h| > 1$  the solution (2.8) holds for any  $C^+$ ,  $C^- \neq 0$ . To make the solution work at  $|h| = 1$ , one requires two boundary conditions that include  $a_1$  and  $a_{-1}$ . These are obtained by considering clock- and counterclockwise round trips around the axis. According to (2.4)

$$a_{-1} = a_{-1}(a_{-2}, a_0, b_{-1}). \quad (2.11)$$

This notation implies that  $a_{-1}$  is expressed through  $a_{-2}$ ,  $a_0$  and  $b_{-1}$ . One continues using the relations (2.4), (2.5) and (2.6) on the right-hand side of (2.11). For example, in the next step, use (2.5) to express  $b_{-1} = b_{-1}(b_0, b_{-2}, a_{-1})$ . It follows an equation

$$a_{-1} = a_{-1}(a_{-2}, a_0, b_0, b_{-2}, a_{-1}). \quad (2.12)$$

Use (2.5) again to substitute for  $b_0$  yielding  $a_{-1} = a_{-1}(a_{-2}, a_0, b_{-1}, b_1, b_{-2}, a_{-1})$ . Next, all  $b_h$  can be expressed in terms of  $a_h$ . It follows

$a_{-1} = a_{-1}(a_{-2}, a_0, a_{-2}, a_{-1}, a_1, a_2, a_{-3}, a_{-1})$ . Finally, with (2.4),  $a_0$  is expressed through  $a_{-1}$  and  $a_1$  yielding the boundary condition

$$\begin{aligned} 0 = & z^6 - z^{12}(1 + y_l^2) - z^6 a_{-3} - z^3(-2 + z^6) a_{-2} \\ & + (-1 + z^6 + z^8 - z^{12}(1 + y_l^2)) a_{-1} \\ & - z^6(-1 + z^6)(1 + y_l^2) a_1 - z^9 y_l^2 a_2. \end{aligned} \quad (2.13)$$

The second boundary condition is obtained analogously by starting with  $a_1 = a_1(a_2, a_0, b_1)$ . It reads

$$\begin{aligned} 0 = & z^{12}(1 + y_l^2) - z^6 y_l^2 + z^9 a_{-2} + z^6(-1 + z^6)(1 + y_l^2) a_{-1} \\ & + (z^{12} + (1 - z^6 - z^8 + z^{12}) y_l^2) a_1 \\ & + z^3(-2 + z^6) y_l^2 a_2 + z^6 y_l^2 a_3. \end{aligned} \quad (2.14)$$

When the Ansatz (2.8) is plugged into the boundary relations (2.13, 2.14), one may solve the equation system for  $C^\pm$ . With the expression for  $a_0$  from (2.4) the generating function becomes

$$\bar{a}(z, y_l) = z a_0 \quad (2.15)$$

$$= z^4 (1 + C^- \lambda_-^{-1} + C^+ \lambda_+). \quad (2.16)$$

The denominator  $D$  of  $\bar{a}$  can be considered a function  $D = D(\lambda_+(z), \lambda_-(z), z, y_l)$  the roots of which are the pole singularities of  $\bar{a}$ . However,  $D(z)$  is a very complicated function of  $z$ , so it seems not possible to determine the roots of  $D$  and thereby the free energy in the corresponding phases. Nevertheless, one may set  $z = z_b$  and determine if there exist values  $y_l^{(c)}$ , so that  $D(z = z_b, y_l^{(c)}) = 0$ . This means that there exists a phase transition from the bulk phase into a phase associated with a pole singularity. At  $z = z_b$ ,  $\lambda_+ = \lambda_- = (1 - z_b^4)/z_b^3$  and as a function of  $y_l$ , the denominator has the form

$$D(z = z_b, y_l) = A_0(z_b) - A_2(z_b) y_l^2 + A_4(z_b) y_l^4, \quad (2.17)$$

where

$$A_0 = 4z_b^{18} (1 + z_b^2 - 6z_b^6 - z_b^8 + z_b^{10}), \quad (2.18)$$

$$\begin{aligned} A_2 = & (1 + z_b^4) \times \\ & \{5 - z_b^4 (17 + 41z_b^2 - 18z_b^4 - 93z_b^6 - 87z_b^8 + 67z_b^{10} \\ & + 100z_b^{12} + z_b^{14} - 54z_b^{16} - 8z_b^{18} + 7z_b^{20})\}, \end{aligned} \quad (2.19)$$

and

$$A_4 = z_b^{12} (-1 + z_b^2)^4 (1 + z_b^2)^2 (1 + 2z_b^2 + 3z_b^4). \quad (2.20)$$

Physical singularities are found when

$$y_l^\pm = \sqrt{\frac{A_2 \pm \sqrt{A_2^2 - 4A_0A_4}}{2A_4}}. \quad (2.21)$$

Let  $\beta_l^\pm = \log y_l^\pm$  and denote by  $z_c^\pm(\beta_l)$  the pole singularities as a function of  $\beta_l$  for which  $z^\pm(\beta_l^\pm) = z_b$ . At  $\beta_l = 0$  the system is in the bulk phase so that the free energy must take the form

$$f(\beta_l) = - \begin{cases} \log z_c^-(\beta_l) & \beta_l < \beta_l^-, \\ \log(z_b) & \beta_l^- \leq \beta_l \leq \beta_l^+, \\ \log z_c^+(\beta_l) & \beta_l > \beta_l^+. \end{cases} \quad (2.22)$$

Numerically, the values approximate to ( $z_b = 0.7167$ )

$$\beta_l^\pm = \pm 1.4045. \quad (2.23)$$

We conclude that we have shown that, at least in principle, weighting the writhe of SAUK can induce a phase transition at a non-trivial value of  $\beta_L$ . This is true, at least when the ensemble of SAP is restricted appropriately. By construction, the high torque phase is associated with the SAUK that wrap around their axis. In the next section we will consider the full ensemble of SAP via simulations.

### 3. Simulations

Self-avoiding lattice knots, including SAUKs have been treated via simulations in the lattice polymer literature before. Most notably in [13], the authors considered SAPs of lengths up to  $2 \times 10^5$  via Markov Chain Monte Carlo (MCMC) simulations, where (effectively) uncorrelated samples were generated with the two-point pivot algorithm. Via a knot detection algorithm, the samples could then be categorized by knot type. Their main result was that the scaling exponent associated with the radius of gyration appears to be invariant when the ensemble of SAP is restricted to a certain knot type. A result that cannot be derived from the renormalization group, as the renormalization group transformation will in general not preserve the knot type.

In this section we want to consider the ensemble of unknotted SAP (SAUK) weighted by their writhe. However, we will not use the same approach as in [13] to sample states via MCMC. There are two reasons for this. First, when the writhe of SAPs is weighted, the ensemble is dominated by increasingly denser states for which the pivot algorithm becomes ineffective. Second, the ensemble becomes increasingly populated by knotted states, thus it becomes hard to sample effectively.

Instead, in this section we solve the model (1.17) via simulations with the Wang-Landau algorithm (WLA) [39] using a local move set that preserves the knot type. In this section, we use  $w = 4Wr$ , which is an integer for a SAP on the sc lattice.

#### 3.1. Algorithm and Data

We use a parallel version of the WLA as discussed for example in [40], but with a maximum of merely eight parallel threads. We initialize an unknotted, rooted SAP on the positive half-space of the sc lattice and generate new states using the pull-moves [41] (excluding the end-move). The pull-moves certainly preserve the knot type of the SAP,

however in contrast to the case of the SAW, to our knowledge, it is not proven that the pull moves are ergodic within the knot type. For some simulations we also used kink transport between random positions. Suppose the current state is  $\varphi$ , then we obtain a state  $\varphi^*$  by applying a move to  $\varphi$ . In order to determine the writhe of  $\varphi^*$ , we rely on the formula (1.9). Therefore, we need to determine the linking number of the SAUK  $\varphi$  with the pushed off unknot  $\varphi + 0.5 (1, 1, 1)^T$ . The linking number can be determined by considering the signed crossing in a projection. Suppose we project the SAUK into the  $x_2$ - $x_3$  plane, then all crossings will occur at potential crossing points of the form  $p_c = (x_2 + 0.5, x_3 + 0.5)$ ,  $x_2, x_3 \in \mathbb{Z}$ . Therefore, every time a bond is added, the two potential crossing points are determined and the bonds are linked to these crossing points via pointers. When there are already bonds linked to the crossing point, we cycle through all perpendicular bonds (that correspond to the pushed off curve or vice versa) and compute the sum of signed crossing that the new bond produces with all the bonds that have already been linked. This corresponds to the change in linking number. The same procedure is performed once a bond is removed. This time however, the linking number changes by the negative of the sum of signed crossings produced by the bond. This algorithm was inspired by [17].

In order to determine the extension (1.16), we keep a list of integer  $N_V[H]$ , which count the number of vertices in the plane  $x_3 = H$ . Then, every time a move removes a vertex  $\varphi_i$  from one position, we update the list as  $N_V[(\varphi_i)_3] \leftarrow N_V[(\varphi_i)_3] - 1$ . The list is modified accordingly when the vertex is placed onto its new position. Finally, every time a list update yields  $N_V[H] = 0$  for some  $H$ , we set the new extension  $h = H$ . We do the same when the population increases from  $N_V[H] = 0$ .

At given length  $n$ , we use the WLA to produce estimates for the quantities

$$s_{wh} := \log C_{wh} \quad (3.1)$$

and

$$s_w(\beta_h) := \log \left( \sum_h C_{wh} e^{\beta_h h} \right). \quad (3.2)$$

Here, estimates means that we obtain (3.1, 3.2) modulo a constant, including a statistical error and possibly a systematic error. In order to obtain the estimate for  $s_w(\beta_h)$  for general  $\beta_h$ , rather than for  $\beta_h = 0$ , we modify the acceptance probability of the canonical WLA. Suppose the current state at time  $t$  is  $\varphi(t)$  and the state  $\varphi^*$  is proposed. Denote writhe and extension of the current state by  $w(t)$  and  $h(t)$ , respectively. For  $\varphi^*$ , denote these as  $w^*$  and  $h^*$ , then, we accept  $\varphi^*$  with the probability

$$P_{acc} = \exp \left\{ s_{w=w(t)}^{(est)}(\beta_h t) - s_{w=w^*}^{(est)}(\beta_h, t) + \beta_h \cdot (h^* - h(t)) \right\}. \quad (3.3)$$

We ran multiple simulations to estimate  $s_{nw}(\beta_h)$  at different lengths  $n$  and stretching forces  $\beta_h$ . We actually produced estimates for  $s_{n|w|}(\beta_h)$  and used the symmetry  $s_w = s_{-w}$  to produce  $s_w(\beta_h)$ . We usually used a cut-off for the writhe, so that  $|w| \leq 0.5n$ . This can be justified because  $s_{nw}(\beta_h)$  falls off quickly towards large  $|w|$ .

This is for example shown in the estimate of the two-dimensional entropy at  $n = 80$  in Figure 3.1. The observables that we are interested in here are the derivatives of the free energy with respect to  $\beta_l$ . We denote the estimates of the derivatives by  $f_n^l$ ,  $f_n^{ll}$ ,  $f_n^{lll}$ . Therefore,

$$f_n^l : = n^{-1} \langle w \rangle_n^{(est)}, \quad (3.4)$$

$$f_n^{ll} : = n^{-1} \left\langle \left( w - \langle w \rangle^{(est)} \right)^2 \right\rangle^{(est)}, \quad (3.5)$$

$$f_n^{lll} = n^{-1} \left( \langle w^3 \rangle^{(est)} - 3 \langle w^2 \rangle^{(est)} \langle w \rangle^{(est)} + 2 \left( \langle w \rangle^{(est)} \right)^3 \right), \quad (3.6)$$

where for example  $\langle w \rangle_n^{(est)} (\beta_l, \beta_h = \text{const})$  can be computed as

$$\langle w \rangle_n^{(est)} (\beta_l, \beta_h = \text{const}) = \frac{\sum_w w e^{\beta_l w + s_n^{(est)} w (\beta_h)}}{\sum_w e^{\beta_l w + s_n^{(est)} w (\beta_h)}}. \quad (3.7)$$

We provide a 95% confidence interval for our results, by obtaining from each simulation several estimates  $s_w$  at different times. We choose the times long enough apart so that the estimates can be considered decorrelated. From each estimate, we compute observables, pretend them to be independent and compute the standard confidence interval.

We note while it is possible to consider other observables like the radius of gyration or the number of contacts by taking sample averages along  $\varphi(t)$ , we will not present such results here. We note that in particular good estimates for the radius of gyration will be good only for short lengths as the local move set requires a long time to decorrelate these observables. Also, since  $\varphi(t)$  is not a Markov process, there is no (canonical) theory of the related error.

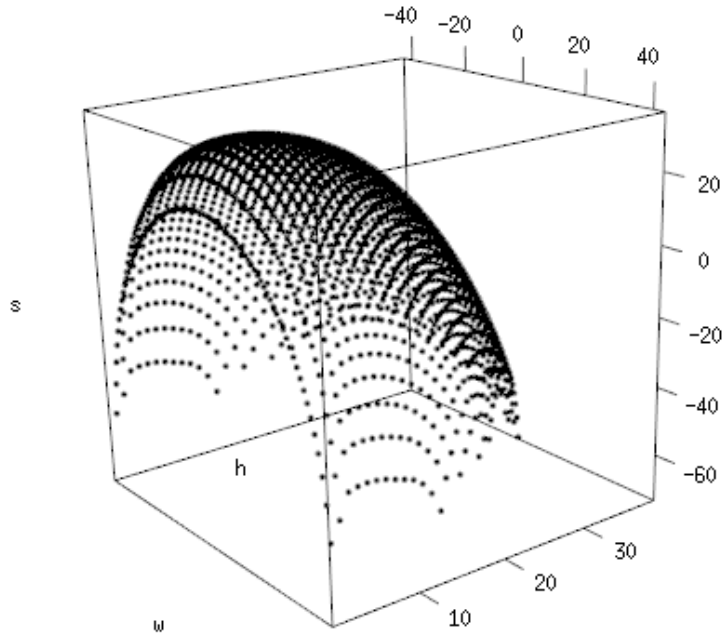


**Figure 3.1.** Two-dimensional entropy  $s$  of the self-avoiding unknot at  $n = 80$  over the extension  $h$  and the writhe  $w = 4Wr$ . This entropy lacks macrostates  $w > 42$  as well as the macro state  $(w = 0, h = 0)$ . The problem of generating samples of planar polygons in three dimensions with the pull moves has been addressed in the appendix of [42].

### 3.2. Results

Figure 3.2 shows writhe fluctuations  $f_n^l(\beta_l, \beta_h)$  at length  $n = 80$ . At  $\beta_h \leq 0$ , the maximum of the writhe fluctuation lies at  $\beta_l = 0$ . As the pulling force is increased, the maximum splits into two modes, where the region between the peaks is expected to be dominated by states with many bonds aligned in force direction. This however suppresses the writhe fluctuations that occur along the polymer.

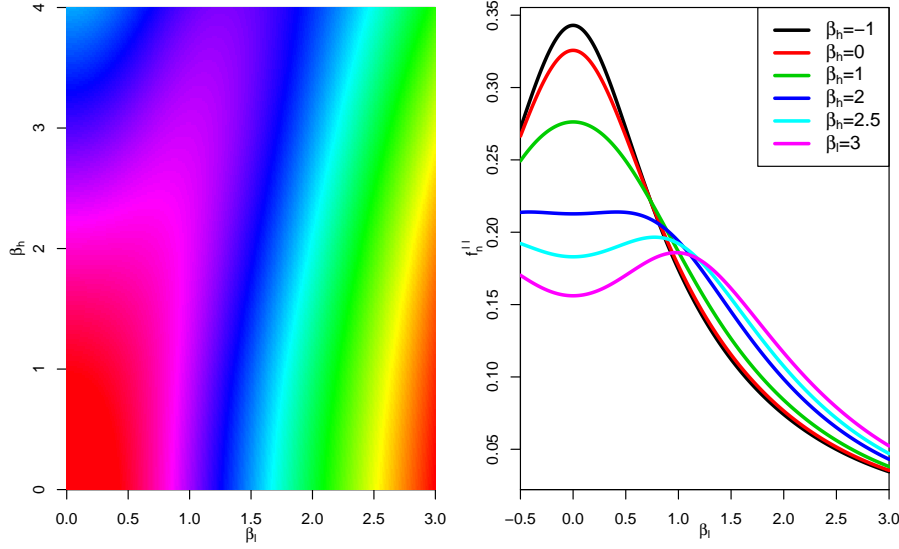


**Figure 3.2.** The graphic on the left-hand side shows a heat plot (rainbow colors) of the writhe fluctuations in the  $\beta_l - \beta_h$ -plane at length  $n = 80$ . The fluctuations are maximal at the origin (violet-red). As  $\beta_h$  is increased, this maximum begins to branch. This is also shown in the graphic on the right-hand side, which shows the writhe fluctuations per length at selected pulling forces  $\beta_h$  against the torque  $\beta_l$ .

At a pulling force of approximately  $\beta_h = 2.5$ , two peaks in  $f''_{n=80}$  (Figure 3.2) appear. Note that this pulling force is small enough so that we do not have to worry about lattice effects from fully extended walks. In fact, the typical extension at  $\beta_l = 0$ ,  $\beta_h = 2.5$  is  $\langle h \rangle_n / n \approx 0.25$  and thus about half of the possible maximum of  $(h_n/n)^{(max)} = (n-2)/(2n)$ . We will focus our analysis on  $\beta_h = 2.5$  which is an intermediate pulling force.

Figure 3.3 shows the scaling of the first and second derivative of the finite size free energy with respect to  $\beta_l$  at  $\beta_h = 2.5$ . While the scaling in the first derivative is rather weak, the peak in the second derivative grows with the length. Also, the rising flank becomes steeper with length. We conjecture that the observed scaling is compatible with a phase transition that sees the second derivative  $f''_n$  become discontinuous, but not divergent, in the thermodynamic limit. This suggests that the third derivative should be considered as it may be divergent at the transition. The rate at which the third derivative diverges is a measure of the intensity of the transition.



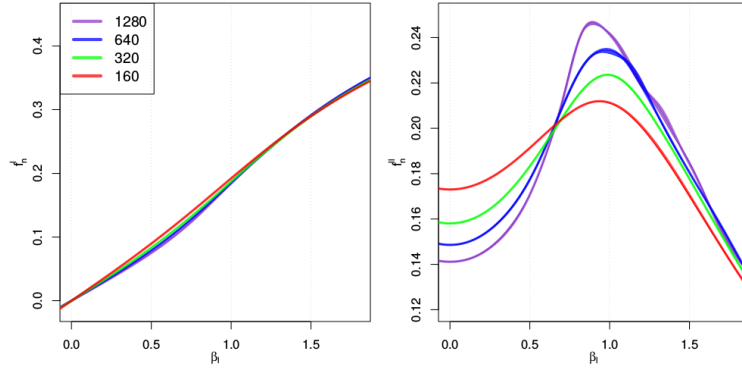


**Figure 3.3.** Scaling of the estimates of the first and second derivative of the free energy  $f_n$  with respect to  $\beta_l$  against  $\beta_l$  at  $\beta_h = 2.5$ .

The third derivatives are shown in the first graph of Figure 3.4. The second graph in Figure 3.4 shows a linear fit to the logarithm of the peak height in  $n f_n^{lll}$  against the logarithm of the length. The slope of this fit is an estimate of the scaling exponent  $\zeta_{lll}$  which is defined by the naively conjectured scaling relation  $f_n^{lll}(\beta_l^{(n)}) \sim n^{\zeta_{lll}-1}$ . The good fit suggests that this Ansatz is correct and we may regard the value of  $\zeta_{lll}^{(est)} (= 1.69(2))$  as a measure of the intensity of the transition (at least when the transition is observed via writhe at finite size). When the standard scaling Ansatz 1.4 applies here,  $\zeta_{lll} - 1$  estimates the crossover exponent at large enough lengths. We note that the results make a value of  $\Phi = 1/2$  plausible.

### 3.3. Phase Diagram

We may regard the peak position in the third derivative as the location of the finite size transition. We use  $n = 640$  as reference length and determine the location of the conjectured finite size transition to lie at  $\beta_l^{640}(\beta_h = 2.5) = 0.67(8)$ . The error corresponds to the torque  $\beta_l$  range for which the confidence interval contains points that lie above the peak of its lower boundary. Also note that for  $n \geq 480$ , we do not observe any shift of the peak location  $\beta_l^{(n)}(\beta_h = 2.5)$ , that lies outside the error. We obtained the locations of the transitions at different  $\beta_h$  to obtain the phase diagram in Figure 3.5, where we have called the phase at high torque 'writhed'.

At values  $\beta_h < 2$  we were unable to obtain good estimates of the third derivative. Also, as  $\beta_h$  decreases all signs of scaling fade out from the second derivative at the considered lengths, so that at  $\beta_h = 0$  the second derivative  $f_n^{ll}$  appears to scale trivially. This can be seen in Figure 3.6 which shows the scaling of the second derivative at different pulling forces.

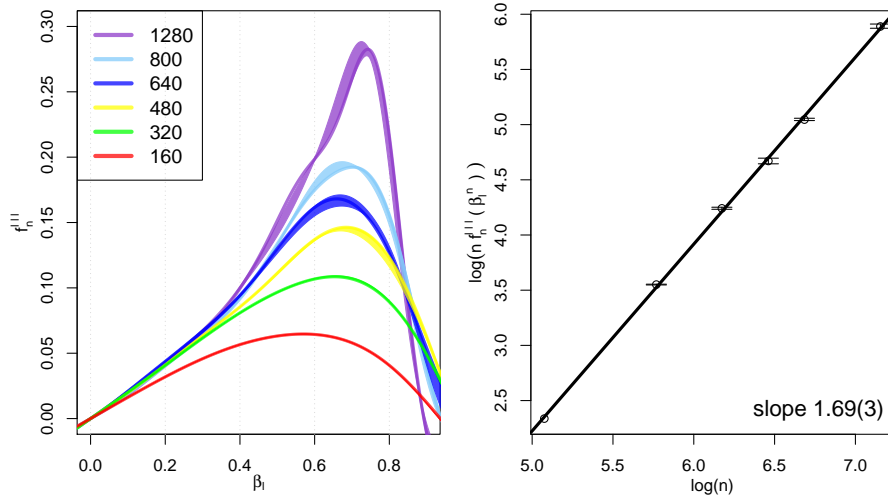


**Figure 3.4.** Left graph: Scaling of the third derivative of the free energy with respect to  $\beta_l$  at  $\beta_h = 2.5$ . Right graph: Values of the maximum in  $n f_n'''(\beta_h = 2.5)$  against the length in log-log-scale. The value of the fit slope is an estimate of the scaling exponent  $\zeta_{III}$  in the Ansatz  $n f_n'''(\beta_l^n) \sim n^{\zeta_{III}}$ .

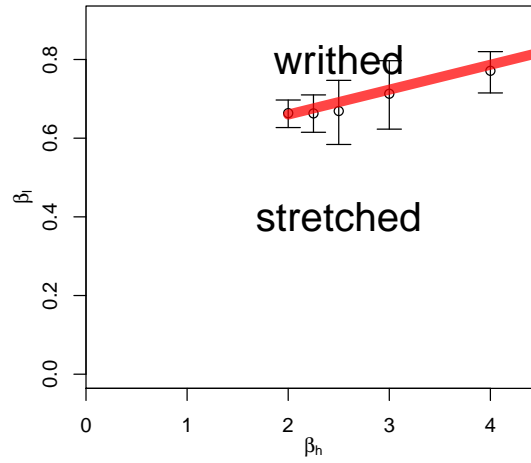


**Figure 3.5.** Phase diagram in the force-torque plane. The red line marks a second-order phase transition. We cannot properly determine the position of the transition for small pulling forces.

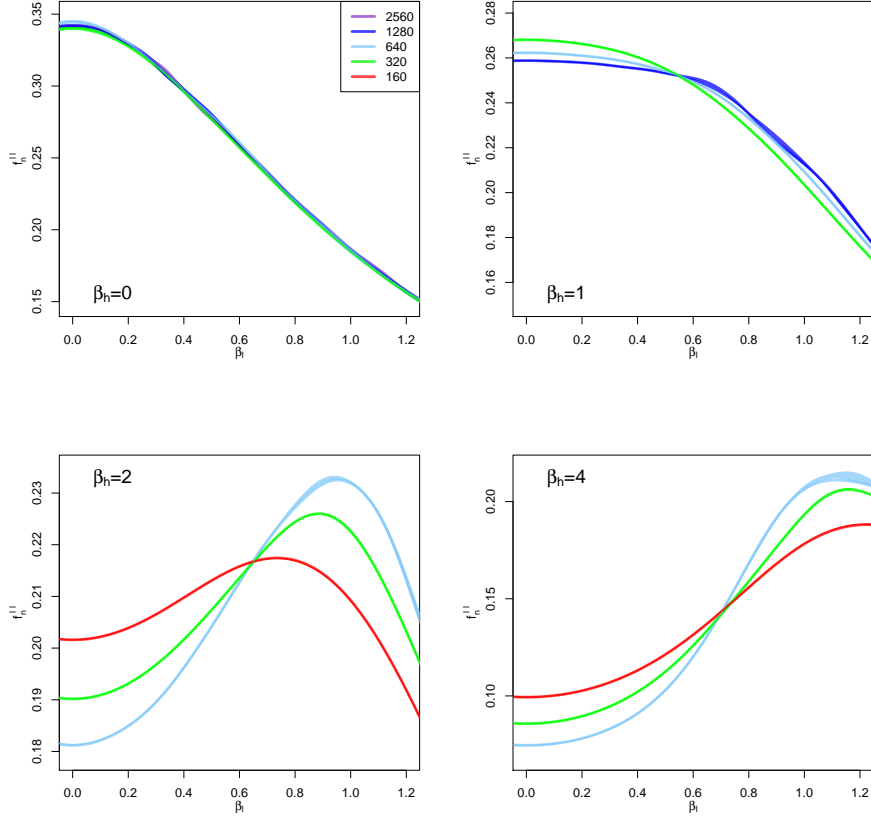


**Figure 3.6.** Scaling of the second derivative of the free energy with respect to  $\beta_l$  at different pulling forces. At  $\beta_h = 0$ , the graph shows the curves for the length  $n = 2580, 1280, 640, 320$ . One cannot make out clear scaling behavior. At  $\beta_h = 1$  the considered lengths are  $n = 1280, 640, 320$ . There is weak non-trivial scaling so that the curve lowest at  $\beta_l = 0$  corresponds to  $n = 1280$  and the upper curve to  $n = 320$ . At  $\beta_h = 2, 4$  the lengths are  $n = 640, 320, 160$  and non-trivial scaling is apparent.

Returning to  $\beta_h = 0$  we report that we have considered lengths of up to  $n = 2560$  and found no scaling. We even probed (not well converged) length  $n = 5120$  and did not see any good indication that non-trivial scaling might start to show. It is likely that then there is no transition when  $\beta_h = 0$ , after all, the pulling force needs to be positive to have stretched phase at high temperatures.

Hence, two scenarios present themselves. Firstly, the stretched to writhed transition exists for all non-zero positive values of  $\beta_h$  and strong corrections to scaling inhibit our ability to detect the transition, or, secondly there exists a minimum value  $\beta_h$  below which the transition does not exist.

Given the form of the writhe fluctuations being maximal around zero it is entirely possible that at small pulling force and short lengths the writhe fluctuations are dominated by a contribution that scales trivially and overpowers the leading non-trivial scaling term. We therefore conclude the first scenario is more likely. However, further work on this is clearly warranted.

### 3.4. The scaling exponent $\zeta_w$

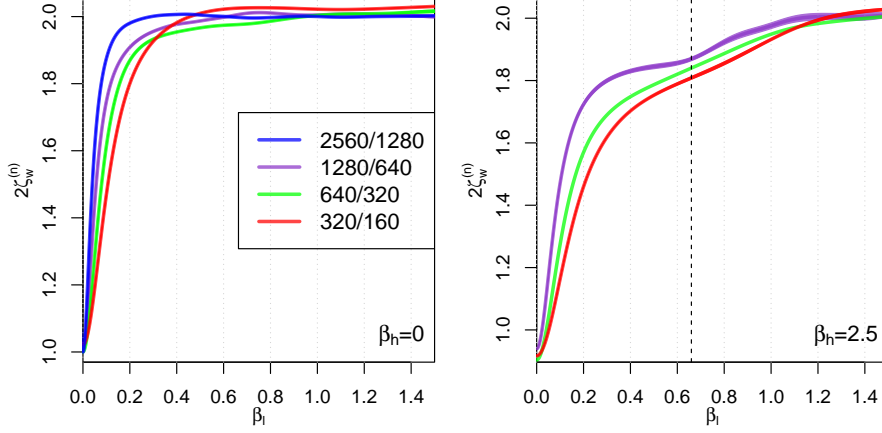


**Figure 3.7.** Estimates for  $2\zeta_w^{(n)}$  against torque at pulling forces  $\beta_h = 0$  and  $\beta_h = 2.5$ . The dotted vertical line lies at  $\beta_l = 0.66$  and marks the location of the transition.

We assume that the squared writhe has the scaling form (1.12), which defines the exponent  $\zeta_w$ . However, because we do not know the corrections to the leading scaling for a SAUK, we define the length dependent exponent  $\zeta_w^{(n)}$  by

$$2\zeta_w^{(n)} = \frac{\log(\langle w^2 \rangle_{2n} / \langle w^2 \rangle_n)}{\log 2}. \quad (3.8)$$

By definition, for large enough  $n$ ,  $\zeta_w^{(n)}$  converges towards  $\zeta_w$  with  $n$ . Figure 3.7 shows the estimate for  $2\zeta_w^{(n)}$  at the pulling forces  $\beta_h = 0$  and  $\beta_h = 2.5$ . At  $\beta_h = 0$ , we do not find any signs that  $2\zeta_w$  behaves different from a trivial case, i.e.  $2\zeta_w(\beta_l = 0) = 1$  and  $2\zeta_w(\beta_l > 0) = 2$ . This re-enforces our conclusion that there is no finite temperature transition when  $\beta_h = 0$ .

With the pulling force  $\beta_h = 2.5$  applied, the estimate for  $2\zeta_w^{(n=640)}$  at  $n = 640$  shows signs of plateauing around 1.85 for small torque. This suggests that the regime  $0 < \beta_l < \beta_l^{(\infty)}$  below the conjectured phase transition might be associated with a scaling exponent  $2\zeta_w < 2$ . Again this aligns with the conclusion above of a transition around  $\beta_l \approx 0.66$  at least when  $\beta_h > 2$ .

Note that without any writhe coupling, that is, for  $\beta_l = 0$  our data is consistent with  $2\zeta_w = 1$  regardless of  $\beta_h$ . In fact, for  $\beta_h = 2.5$  the estimates for  $2\zeta_w^{(n)}$  all lie slightly below one when  $\beta_l = 0$ . From a scaling point of view it is unlikely that the asymptotic value of  $2\zeta_w$  actually lies below 1 but that finite length estimates are affected by different corrections to scaling as  $\beta_l$  is varied.

#### 4. Conclusion

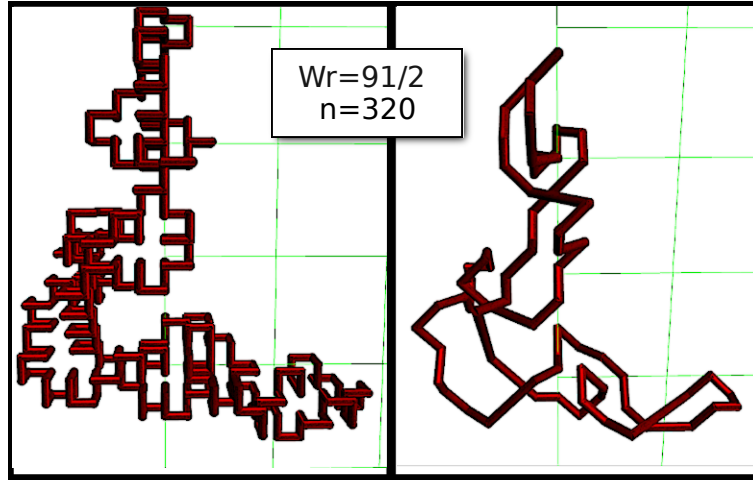


**Figure 4.1.** A state  $\varphi$  of high writhe ( $w = 182$ ) at length  $n = 320$  on the sc lattice (left). The picture on right-hand side was obtained by removing all kinks in  $\varphi$  and cutting across all remaining right angles. This procedure makes the global geometry more visible and shows that SAUK wraps around itself.

In this paper we weighted the writhe of unknotted SAPs on the sc lattice to identify potential phase transitions, as this can be related to experiments that turn DNA. In Section 1, we pointed out that the writhe can be considered both a partly global and partly local quantity. While we do not expect a phase transition in an ensemble of SAUK where the writhe can be considered to be local, we have defined in Section 2 a subset of SAUK for which the writhe must be considered global. That is, most of the writhe must be determined by relating distant bonds of the SAP to each other. Via an exact solution we found the existence of a phase transition at  $\beta_l \approx 1.4$ , where by construction we expect the SAP to transition into a phase where it wraps around its axis. We have considered this as a very simplified toy model of a SAUK that is being pulled strongly.

We considered the full problem in Section 3 via simulations with the WLA. When the SAP is pulled sufficiently, we provided results that are compatible with a second-order phase transition at which the writhe fluctuations per length jump by a finite amount as the critical torque  $\beta_l^\infty$  is approached from below in the thermodynamic limit. We refer to the conjectured phase at high torque as “writhed”. At low torques the SAP is in a stretched phase with anisotropic size scaling. As the pulling force was reduced, we observed that the scaling in the writhe fluctuations fades out, so that at zero pulling force  $\beta_h = 0$ , we do not find any signs of scaling. While one might conclude that for pulling forces smaller than some force  $\beta_h^*$  the transition either no longer exists or changes its universality class, it is more likely that it is necessary to study longer and longer lengths as  $\beta_h$  approaches zero. At  $\beta_h = 0$  we do not see any transition and this conclusion is re-enforced by considering the scaling exponent  $2\zeta_w$  of the squared

writhe. We also considered the scaling exponent  $2\zeta_w$  associated with the squared writhe at non-zero pulling force. We observed a possible plateauing of  $2\zeta_w^{(n)}$  ( $\beta_h = 2.5$ ) to a value of  $2\zeta_w$  falls below 2 but larger than 1 for large  $\beta_h > 0$  at small  $\beta_l > 0$ . Now the finite length estimates below the transition are still increasing and it is entirely possible that  $2\zeta_w = 2$  for all  $\beta_l$ . It would then be a change in corrections to the scaling of  $2\zeta_w$  that signals the transition. It is certainly unclear how such a non-trivial value might originate so that further study is required.

## Acknowledgments

One of the authors, ED, gratefully acknowledges the financial support of the University of Melbourne via its Melbourne International Research Scholarships scheme. Financial support from the Australian Research Council via its support for the Centre of Excellence for Mathematics and Statistics of Complex Systems and the Discovery Projects scheme is gratefully acknowledged by one of the authors, ALO, who also thanks the School of Mathematical Sciences, Queen Mary University of London for hospitality. ED also acknowledges support from VLSCI HPC, Edward HPC and the School of Mathematics and Statistics at the University of Melbourne for providing computational resources.

## References

- [1] T. Strick, J.-F. Allemand, V. Croquette, and D. Bensimon. Twisting and stretching single DNA molecules. *Progress in Biophysics and Molecular Biology*, 74(1-2):115 – 140, 2000.
- [2] T. R. Strick, Allemand J.-F., D. Bensimon, A. Bensimon, and V. Croquette. The elasticity of a single supercoiled DNA molecule. *Science*, 271(5257):1835, 1996.
- [3] S. B. Smith, L. Finzi, and C. Bustamante. Direct mechanical measurements of the elasticity of single DNA molecules by using magnetic beads. *Science*, 258(5085):1122–1126, 1992.
- [4] S. Forth, C. Deufel, M. Y. Sheinin, B. Daniels, J. P. Sethna, and M. D. Wang. Abrupt buckling transition observed during the plectoneme formation of individual DNA molecules. *Physical Review Letters*, 100:148301, 2008.
- [5] H. Brutzer, N. Luzzietti, D. Klaue, and R. Seidel. Energetics at the DNA supercoiling transition. *Biophysical Journal*, 98(7):1267, 2010.
- [6] C. Deufel, S. Forth, C. R. Simmons, S. Deigsha, and M. D. Wang. Nanofabricated quartz cylinders for angular trapping: DNA supercoiling torque detection. *Nature Methods*, 4(3):223 – 225, 2007.
- [7] F. Mosconi, J. F. Allemand, D. Bensimon, and V. Croquette. Measurement of the torque on a single stretched and twisted DNA using magnetic tweezers. *Physical Review Letters*, 102(7):078301, 2009.
- [8] A. Sokal. Critical exponents, hyperscaling, and universal amplitude ratios for two- and three-dimensional self-avoiding walks. *Journal of Statistical Physics*, 80(3-4):661, 1995.
- [9] N. Clisby. Accurate Estimate of the Critical Exponent  $\nu$  for Self-Avoiding Walks via a Fast Implementation of the Pivot Algorithm. *Physical Review Letters*, 104(5):055702, 2010.
- [10] F. Valle, M. Favre, P. De Los Rios, A. Rosa, and G. Dietler. Scaling exponents and probability distributions of DNA end-to-end distance. *Physical Review Letters*, 95(15):158105, 2005.
- [11] A. L. Owczarek, J. W. Essam, and R. Brak. Scaling analysis for the adsorption transition in a watermelon network of  $n$  directed non-intersecting walks. *Journal of Statistical Physics*, 102:997 – 1018, 2001.

- [12] E. J. J. Rensburg, E. Orlandini, D. W. Sumners, M. C. Tesi, and S. G. Whittington. The Writhe of a self-avoiding polygon. *Journal of Physics A: Mathematical and General*, 26(19):L981 – L986, 1993.
- [13] M. Baiesi and E. Orlandini. Universal properties of knotted polymer rings. *Physical Review E*, 86(3-1):1 – 7, 2012.
- [14] C. Micheletti, D. Marenduzzo, E. Orlandini, and D. W. Sumners. Knotting of random ring polymers in confined spaces. *Journal of Chemical Physics*, 124(6):064903, 2006.
- [15] M. Baiesi, E. Orlandini, and S. G. Whittington. Interplay between writhe and knotting for swollen and compact polymers. *Journal of Chemical Physics*, 131(15):154902, 2009.
- [16] M. Baiesi, E. Orlandini, and A. L. Stella. Ranking knots of random, globular polymer rings. *Physical Review Letters*, 99(5), 2007.
- [17] R. C. Lacher and F. B. Sumners. Data structures and algorithms for computation of topological invariants of entanglements: Link, Twist, Writhe. In R.J.Roe, editor, *Computer Simulation of Polymers*, pages 365–373. Prentice-Hall, Englewood Cliffs, NJ, 1991.
- [18] C. Laing and D. W. Sumners. Computing the writhe on lattices. *Journal of Physics A: Mathematical and General*, 39(14):3535, 2006.
- [19] P. K. Agarwal, H. Edelsbrunner, and Y. Wang. Computing the writhing number of a polygonal knot. *Discrete and Computational Geometry*, 32:37–53, 2004.
- [20] J. Aldinger, I. Klapper, and M. Tabor. Formulae for the calculation and estimation of writhe. *Journal of Knot Theory and Its Ramifications*, 32:37–53, 1995.
- [21] E. Dagrosa and A. L. Owczarek. Generalizing ribbons and the twist of the lattice ribbon. *Journal of Statistical Physics*, 155:392 – 417, 2014.
- [22] W. Kung and R. D. Kamien. Topological constraints at the theta-point: Closed loops at two loops. *Europhysics Letters*, 64(3):323 – 329, 2003.
- [23] E. Dagrosa, A. L. Owczarek, and T. Prellberg. Writhe-induced knotting in a lattice polymer. *Journal of Physics A: Mathematical and Theoretical*, 48(6):065002, 2015.
- [24] W. Kung and R. D. Kamien. Topological constraints at the theta-point: Closed loops at two loops. *Europhysics Letters*, 64:323 – 329, 2003.
- [25] J. Cantarella, D. DeTurck, and H. Gluck. Upper bounds for the writhing of knots and the helicity of vector fields. *AMS IP Studies in Advanced Mathematics*, 24:1 – 22, 2001.
- [26] E. Orlandini and E. Janse van Rensburg. Twist in an exactly solvable directed lattice ribbon. *Journal of Statistical Physics*, 80:781–791, 1995.
- [27] S. Sinha and J. Samuel. Statistical mechanics of ribbons under bending and twisting torques. *Journal of Physics: Condensed Matter*, 25(46):465102, 2013.
- [28] F. B. Fuller. Decomposition of the linking number of a closed ribbon: A problem from molecular biology. *Proceedings of the National Academy of Sciences*, 75(8):3557–3561, 1978.
- [29] S. Sinha and J. Samuel. Biopolymer elasticity: Mechanics and thermal fluctuations. *Physical Review E*, 85:041802, 2012.
- [30] J. Samuel and S. Sinha. Molecular elasticity and the geometric phase. *Physical Review Letters*, 90:098305, 2002.
- [31] J. Samuel and S. Sinha. Tops and writhing DNA. *Journal of Statistical Physics*, 143(2):399 – 412, 2011.
- [32] J. Samuel, S. Sinha, and A. Ghosh. Comment on "Writhe formulas and antipodal points in plectonemic DNA configurations". *Physical Review E*, 80(6 Pt 1):063901; discussion 063902, 2009.
- [33] C. Bouchiat and M. Mezard. Elastic rod model of a supercoiled DNA molecule. *The European Physical Journal E*, 2(4):377–402, 2000.
- [34] J. H. White. Self-linking and the Gauss integral in higher dimensions. *American Journal of Mathematics*, 91(3):pp. 693–728, 1969.
- [35] G. Călugăreanu. Sur les classes d'isotopie des noeuds tridimensionnels et leurs invariants. *Czechoslovak Mathematical Journal*, 11:588–625, 1961.

- [36] G. Călugăreanu. Sur les enlacements tridimensionnels des courbes fermées. *Communications of the Academia Republicii Populare Romîne*, 11:829–832, 1961.
- [37] J. Krawczyk, A. L. Owczarek, T. Prellberg, and A. Rechnitzer. Pulling absorbing and collapsing polymers from a surface. *Journal of Statistical Mechanics: Theory and Experiment*, 2005(05):P05008, 2005.
- [38] R. Brak, G. K. Iliev, A. L. Owczarek, and S. G. Whittington. The exact solution of a three-dimensional lattice polymer confined in a slab with sticky walls. *Journal of Physics A: Mathematical and Theoretical*, 43(13):135001, 2010.
- [39] F. Wang and D. P. Landau. Efficient, multiple-range random walk algorithm to calculate the density of states. *Physical Review Letters*, 86:2050–2053, 2001.
- [40] Y. W. Li, T. Vogel, T. Wuest, and D. P. Landau. A new paradigm for petascale Monte Carlo simulation: Replica exchange Wang-Landau sampling. *Journal of Physics: Conference Series*, 510(1):012012, 2014.
- [41] N. Lesh, M. Mitzenmacher, and S. Whitesides. A complete and effective move set for simplified protein folding. In *Proceedings of the seventh annual international conference on Research in computational molecular biology*, Recomb '03, pages 188–195, New York, NY, USA, 2003. ACM.
- [42] A. Swetnam and C. Brett and M. .P. Allen. Phase diagrams of knotted and unknotted ring polymers *Physical Review E*, 85:031804, 2012.